

# High-speed train positioning based on a combination of Beidou navigation, inertial navigation and an electronic map

Hui YANG<sup>1,2,3\*</sup>, Shuai-Qiang DONG<sup>1,2,3</sup> & Chun-Hua XIE<sup>1,2,3</sup><sup>1</sup>*School of Electrical and Automation Engineering, East China Jiaotong University, Nanchang 330013, China;*<sup>2</sup>*Key Laboratory of Advanced Control & Optimization of Jiangxi Province, East China Jiaotong University, Nanchang 330013, China;*<sup>3</sup>*State Key Laboratory of Performance Monitoring Protecting of Rail Transit Infrastructure, East China Jiaotong University, Nanchang 330013, China*

Received 23 May 2022/Revised 7 August 2022/Accepted 3 November 2022/Published online 29 June 2023

**Abstract** To date, the studies on the combination positioning of high-speed trains have made great progress, but the positioning accuracy of these methods is relatively low. Map-matching positioning can improve positioning accuracy, but information transmission is time-consuming. Few studies incorporate it into combination positioning. To solve the problem, this paper proposes a high-speed train positioning method based on combining a Beidou navigation system, an inertial navigation system, and an electronic map. First, the combination positioning problem is transformed into a multi-objective optimization problem, which weights the direction similarity and distance error to form a fitness function and converts the railway line and the maximum error range of each positioning system into constraints. Second, an improved differential evolution algorithm is proposed to solve this problem. By referencing the gray wolf algorithm, the differential evolution algorithm updates individuals by varying toward the direction of multiple optimal values. Then, a new combination positioning algorithm for high-speed trains is proposed. In the simulation, the increase in positioning speed and accuracy is analyzed and validated. Compared to the current algorithms, the proposed algorithm performs better. The proposed method has practical value for improving the reliability and safety of train operations.

**Keywords** electronic map, multi-objective optimization, differential evolution algorithm, Beidou navigation system, high-speed train positioning

**Citation** Yang H, Dong S-Q, Xie C-H. High-speed train positioning based on a combination of Beidou navigation, inertial navigation and an electronic map. *Sci China Inf Sci*, 2023, 66(7): 172207, <https://doi.org/10.1007/s11432-022-3659-2>

## 1 Introduction

The railroad transportation industry is a pillar of our national economy. With the rapid development of railroad transportation, how to improve efficiency, ensure safety, and reduce the cost of transportation has become a new problem of rail transit [1]. The effective way to solve this problem is to realize continuous autonomous positioning and establish a more advanced and intelligent train control system. Moreover, the autonomous continuous positioning of trains is a prerequisite for building a safe, convenient, efficient, economical, and environmentally friendly railroad transportation network. Because a single positioning system cannot guarantee the continuous real-time positioning of trains, the combination positioning methods of satellite navigation and other positioning technologies have attracted considerable attention from scholars worldwide. The recent studies can be divided into four categories: multi-sensor information fusion, wireless sensor networks, heuristic algorithms, and electronic map-matching.

Multi-sensor information fusion positioning refers to finding the position of high-speed trains by combining the measurement information of each sensor according to certain criteria. The existing studies

---

\* Corresponding author (email: [yhshuo@263.net](mailto:yhshuo@263.net))

mainly address the combined positioning of the inertial navigation system and other sensor systems [2–4]. With the development of communication technology, wireless sensor network positioning was proposed. The wireless sensor network is a distributed sensing network comprising sensors or communication base stations distributed along a railroad line and receiving devices on a train. To explore the positioning of wireless sensor networks, a combined strapdown inertial navigation system (SINS) and radio frequency identification (RFID)-based technology was proposed in [5], and a positioning method combining Beidou satellite navigation technology with GSM-R technology was proposed in [6]. With the increasing variety of information in combination positioning, many scholars have begun to use heuristic algorithms in positioning solving. Borenovic used a GSM and cascade-connected ANN structures to position the vehicle [7]. To solve the problems of low accuracy and poor real-time performance in train positioning, Yang et al. [8] proposed a train combination positioning method based on a gray neural network. The data of these studies come from various positioning systems, but rarely involve electronic map information. Some studies have used electronic map information in the form of map-matching algorithms for positioning. For example, Liu et al. [9] proposed a map-matching method based on the geometric features of the road by combining the characteristics of the continuous and obvious trajectories of actual traffic. Li et al. [10] proposed a precise alignment algorithm for inertial navigation between travels based on map-matching assistance. However, these map-matching algorithms only correct the positioning results of other positioning methods rather than adding electronic map information to the combined positioning information. This method will cause delays in the positioning, and all errors in the electronic map will be presented in the final positioning results. In this paper, the electronic maps are transformed into constraints and added to the combined positioning process, which can improve the efficiency of the high-speed train positioning and attenuate the effect of electronic map drawing errors on the positioning results.

The map-matching method used in [9, 10] is a curve-to-curve map-matching method, that is, first, connecting several consecutive track points of the vehicle to form a curve, then extracting the feature information of the trajectory curve and comparing it with the curve feature information of the electronic map, and finally matching the vehicle to the most similar electronic map segment. However, Ref. [11] stated that this technique is not suitable for high-speed train positioning because most high-speed train tracks are straight and have fluent curves. In addition, Ref. [12] noted the following problems with the direct projection matching method. (1) The projection map-matching method requires accurate electronic maps. If the error in the electronic map is relatively large, the positioning accuracy of map-matching will be reduced. (2) If each measurement point is searched for the nearest point in the electronic map, more time will be consumed, and the real-time requirement of positioning will not be met. (3) The direct projection map-matching method only eliminates errors in the vertical orbit direction, so when the data measured by the Beidou satellite navigation are incorrect, several data points may suddenly be spanned in the electronic map, thus causing map-matching errors.

The current direct projection has the disadvantages of low matching accuracy, poor reliability, computational complexity, and low efficiency, so it cannot meet the actual demands of positioning. Particularly, when the satellite signal is poor, the accuracy of the matching algorithm will be greatly reduced. Compared with existing research methods, the main innovations and differences of this paper are as follows. First, unlike [9, 10], electronic maps are used as constraints in this paper. This approach allows the final positioning results to be within a small area of the electronic map rather than above the track. This method can attenuate the effect of electronic map drawing errors on the positioning results. In contrast to most of the present methods, which use the Kalman filter algorithm for map-matching [13, 14], this paper converts the positioning problem into a multi-objective optimization problem and uses an objective optimization algorithm to solve it. Meanwhile, the positioning information is weighted with the inverse squares of the maximum errors when setting up the objective function. If the error of a particular positioning system becomes larger, its weight factor in the objective function becomes smaller. When a single positioning system fails, this approach reduces its impact on subsequent positioning results.

To add electronic map information to combined positioning data, this paper proposes a high-speed train positioning method based on the combination of a Beidou navigation system, an inertial navigation system, and an electronic map. The main contributions of this paper are as follows.

(a) First, according to the new method, the fusion positioning problem is creatively transformed into a multi-objective optimization problem with multiple constraints, which provides a new solution idea for fusion positioning.

(b) The idea of adding electronic map information as orbit constraints to the combination positioning process is proposed, which will not only save the data transmission time from other positioning modes

to the map-matching algorithm but also improve the real-time performance of fusion positioning.

(c) By combining the gray wolf algorithm and differential evolution algorithm, a new high-speed train positioning algorithm based on map-matching (the GWDE-MM algorithm) is proposed. The new algorithm improves the variation strategy of the differential evolution algorithm, and it can be used in data fusion positioning to enhance the accuracy level.

## 2 Principle of the map-matching

Map-matching is an auxiliary positioning method. By matching the positioning results of other positioning systems with electronic track maps, map-matching can eliminate errors in the longitudinal direction of the railway and achieve more accurate positioning. The geometry matching algorithm is the most basic map-matching algorithm, including point-to-point, point-to-line, and line-to-line matching methods [15]. Accurate electronic maps, high-precision positioning data, and perfect map-matching algorithms are effective means to improve positioning accuracy.

### 2.1 Establishment of an electronic map

In [15], it is mentioned that railway lines have one dimension, and the current track lines can be divided into straight lines, circular curves, and cubic parabolic transition curves. Therefore, the electronic map model for the railway is established as follows:

$$f(x) = \begin{cases} a_1x + b_1, & \text{straight line,} \\ a_2x^2 + b_2x + c_2, & \text{circular curve,} \\ a_3x^3 + b_3x^2 + c_3x + d_3, & \text{transition curve,} \end{cases} \quad (1)$$

where  $x$  is the horizontal coordinate,  $f(x)$  is the corresponding vertical coordinate, and the remains are equation coefficients.

**Remark 1.** The method mentioned here is a theoretical fitting method, and the specific fitting model will be changed according to the fitting error and residual value.

### 2.2 Processing of the positioning data

The positioning data obtained by the satellite positioning system include latitude and longitude coordinate points, while the inertial navigation system obtains plane coordinate data. Therefore, the data should be projected and transformed before map-matching so that the positioning data obtained from satellite navigation and inertial navigation can be unified in the same map.

In this paper, the projection transformation of coordinates is performed by the orthogonal conic projection (Lambert projection) [16, 17]. The idea assumes that a positive cone is tangent or cuts into the Earth's sphere, uses equiangular conditions to project the Earth's sphere onto the cone surface, and then expands the projected Earth's sphere into a planar map along the bus bar.

**Remark 2.** The orthogonal conic projection applies to the drawing of medium- and small-scale maps in mid-latitude areas that are distributed along the latitudes, and it is also a common map projection for drawing domestic maps.

After the projection, the latitude lines are concentric arcs, and the longitude lines are concentric radii. The map is projected without angular distortion. Moreover, the lengths of longitude lines and latitude lines change in equal proportion. The projection deformation is independent of the longitude, and the deformation along the longitude direction is small. The projection length ratio of the tangent conic projection is calculated as follows:

$$m = \frac{\beta\rho}{N\cos B}, \quad (2)$$

where  $\beta = \sin B_0$ ,  $N = a/\sqrt{1 - e^2\cos^2 B}$ ,  $\rho = \rho_0 e^{\beta(q-q_0)}$ ,  $q = \frac{1}{2} \ln \frac{1+\sin B}{1-\sin B} - \frac{e}{2} \ln \frac{1+\sin B}{1-\sin B}$ , and  $\rho_0 = N_0 \cos B_0$ .  $m$  is the projection length ratio,  $B$  is the mean latitude of the edge to be found,  $B_0$  is the standard latitude,  $\beta$  is the constant coefficient determined by Lambert,  $N$  is the radius of curvature of the unitary circle corresponding to the edge to be found,  $\rho$  is the polar distance of the latitude line of the edge to be sought,  $\rho_0$  is the polar distance of the standard latitude line,  $a$  is the length of the Earth's equatorial radius, and  $e$  is the eccentricity of the ellipse corresponding to the standard latitude.

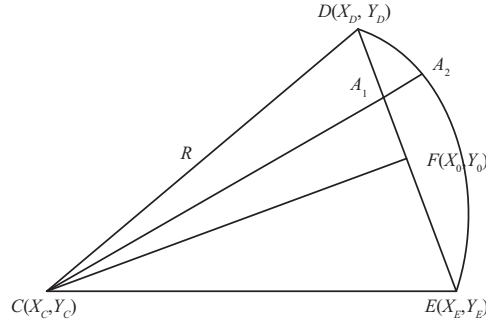


**Figure 1** Positioning method of the circular curve matching.

### 2.3 Algorithm for matching positioning

Most algorithms use direct projection for map-matching. The direct projection method makes a plumb line from the pending position to the map track and considers the intersection as the final positioning point.

**Remark 3.** In the map-matching algorithm, the electronic map is generally considered accurate when the matching algorithm is designed, and the following positioning methods for the gentle curve and circular curve sections are also based on this premise.

For transition curves, the matching algorithm connects the two known points closest to the reference point and passes the vertical line of the connection through the reference point. The intersection of the vertical line and the transition curve is the projection point, and the specific method can be found in [18,19].

For the circular curve part, the matching positioning schematic is shown in Figure 1. The segment  $CF$  vertically bisects the segment  $DE$ . Then, the matching projection point can be found in the following way.

The equation of the line  $CF$  obtained from the coordinates of the points  $C$  and  $F$  is as follows:

$$Y - Y_0 = K_1(X - X_0), \tag{3}$$

where  $X_0 = (X_D - X_E)/2$ ,  $Y_0 = (Y_D - Y_E)/2$ , and  $K_1 = (X_D - X_E)/(Y_D - Y_E)$ .

According to the Pythagorean theorem, triangle  $CFD$  should obey the following formula:

$$|CF|^2 + |DF|^2 = R^2. \tag{4}$$

Assume that the equation of the circle  $C$  is as follows:

$$(X_C - X_0)^2 + (Y_C - Y_0)^2 + \frac{(X_D - X_E)^2 + (Y_D - Y_E)^2}{4} = R^2. \tag{5}$$

By combining (5) with (3), one has

$$X_C = X_0 \pm \sqrt{\frac{R^2 - \frac{d^2}{4}}{1 + K_1^2}}, \quad Y_C = Y_0 \pm \sqrt{\frac{R^2 - \frac{d^2}{4}}{1 + \frac{1}{K_1^2}}}, \tag{6}$$

where  $d^2 = (X_D - X_E)^2 + (Y_D - Y_E)^2$ .

The equations of the line  $CA_1$  and circle  $C$  are assumed as follows:

$$Y_C - Y = \frac{Y_{A_1} - Y_C}{X_{A_1} - X_C}(X_C - X), \tag{7}$$

$$(X_C - X)^2 + (Y_C - Y)^2 = R^2. \tag{8}$$

By solving (7) in conjunction with (8), one has

$$X_{A_2} = X_C \pm \sqrt{\frac{R^2}{1 + \left(\frac{Y_{A_1} - Y_C}{X_{A_1} - X_C}\right)^2}}, \quad Y_{A_2} = Y_C \pm \sqrt{\frac{R^2}{1 + \left(\frac{X_{A_1} - X_C}{Y_{A_1} - Y_C}\right)^2}}. \tag{9}$$

### 3 Transformation of the positioning problem

The information fusion positioning of trains is the process of solving the position estimation of trains, which is based on available satellite positioning information and measurement data from each sensor. In the solution process, multiple minimum errors are usually sought within a certain range, and the final estimated positions are determined by comparing the various solutions. To turn the positioning problem into a multi-objective optimization problem, this paper focuses on population initialization, objective function design, and constraint establishment.

#### 3.1 Initialization of the population

In this paper, the positioning information of the inertial navigation and satellite navigation systems is used for combination positioning. Satellite positioning in urban areas, tunnels, and other areas may cause large positioning errors or even invalid positioning results. Although the problem of error accumulation exists in the positioning of the inertial navigation system, the short-period inertial navigation positioning is relatively accurate. Therefore, this paper assumes that the inertial navigation system can provide continuous positioning, and the initialization of the population is accomplished by adding a random value within the margin of error to the estimated position of the inertial navigation system.

$$pp(i, t) = s(t) + (r - 0.5)\max(e_1), \quad (10)$$

where  $pp(i, t)$  is the  $i$ -th initial individual randomly generated for the  $g$ -th position,  $s(t)$  is the  $t$ -th inertial navigation reference positioning coordinate,  $r$  is a 3-dimensional column vector randomly generated between  $(0, 1)$ , and  $\max(e_1)$  is the maximum inertial navigation error value before the  $t$ -th positioning.

After completing the  $t$ -th positioning, the population is iteratively searched for the optimal estimated position. Then, the parameters of the inertial navigation system and the satellite navigation system are corrected by their coordinate data. The parameter corrections include the following features. For the inertial navigation system, the position, velocity, and acceleration measured by the inertial navigation system are updated with the positioning data obtained by the GWDE-MM algorithm, and the next positioning is calculated based on the best positioning data. For the satellite positioning system, the latitude and longitude of the GWDE-MM positioning are used to subtract the latitude and longitude of the satellite positioning to obtain the offset. In the next positioning, the offset is used to process the positioning result of the Beidou satellite to reduce the positioning error. Finally, the best-estimated position is used as a new position and is used to calculate the next inertial navigation reference position.

#### 3.2 Design of the objective function

A reasonable objective function is more conducive to a quick optimization search of differential evolution algorithms. For the train positioning problem, the positioning objectives can be divided into two aspects. On the one hand, the distance error is minimized. On the other hand, the directional error is minimized. Common methods for solving multi-objective optimization problems include the particle swarm optimization algorithm [19], the differential evolution algorithm (DE) [20], the pigeon-inspired optimization algorithm [21–23], and the gray wolf algorithm (GW) [24]. In [25], the fitness function of the multi-objective genetic algorithm was formed by weighting the spatial similarity, the modified shortest path, and the directional similarity. Referring to this method, the directional similarity and distance errors are weighted to form the fitness function, and the multi-objective function is transformed into a single objective function to solve.

**Remark 4.** Ref. [25] focused on matching floating vehicle positioning points to the correct road, while the present paper focuses on the data fusion positioning of trains, both of which are multi-objective functions, so the multi-objective is converted into a single-objective solution with reference to its method.

The Beidou satellite navigation system is an absolute positioning system, and the magnitude and direction of its errors are uncertain each time. Therefore, satellite positioning mainly provides an error function of the distance value. However, the magnitude and direction of the inertial navigation system errors are related to the positioning result of the previous moment. Hence, the inertial navigation system provides a distance error function and an orientation error function.

The fitness function obtained from the Beidou satellite navigation system is as follows:

$$f_1 = ||pp(i, t) - sp(t)||, \quad (11)$$

where  $sp(t)$  represents the coordinates of the  $t$ -th satellite navigation system reference position.

Similarly, the fitness functions obtained from the distance error and the direction error of the inertial navigation system are as follows:

$$f_2 = ||pp(i, t) - s(t)||, \tag{12}$$

$$f_3 = ||\phi_{pp(i,t)s(t-1)} - \phi_t||, \tag{13}$$

where  $\phi_{pp(i,t)s(t-1)}$  is the orientation error of the  $i$ -th initial individual randomly generated at the  $t$ -th position relative to the  $(t - 1)$ -th inertial navigation system reference positioning coordinate, and  $\phi_t$  represents the orientation change measured by the inertial navigation system.

The errors of inertial navigation systems accumulate over time. Therefore, if the weight value is set to a constant value, a worse positioning effect with error accumulation will be obtained. This paper uses the inverse squares of the maximum errors as the weight coefficients to avoid this situation. The inverse squares of the maximum error are used for weighting because of two considerations. First, to ensure that different positioning systems have the same impact on the fused positioning results, they are normalized, i.e., the current error is divided by the maximum error that has occurred; second, to ensure that the fused positioning system can be positioned relatively well in the event of a sudden system failure, it is weighted by the inverses of the maximum error that has occurred. In summary, the inverse squares of the corresponding maximum error are used as the weight of the individual objective function to form the final objective function. After weighting, the objective function of the map-matching algorithm based on the differential evolution algorithm (DE-MM) is as follows:

$$F(t) = \frac{1}{(e_s^{\max})^2} f_1 + \frac{1}{(\max(e_1))^2} f_2 + \frac{1}{(\max(e_2))^2} f_3, \tag{14}$$

where  $F(t)$  is the fitness function,  $e_s^{\max}$  is the maximum error range value for satellite positioning, and  $\max(e_1)$  and  $\max(e_2)$  are the maximum distance error and directional error value before the  $t$ -th positioning of the inertial navigation system.

**Remark 5.** This approach is advantageous because the weights are adaptively reduced when the error increases, which prevents the positioning system from continuously relying on a particular system. This weighting method ensures that the larger the error in a positioning system, the less impact it will have on the positioning results.

### 3.3 Design of the constraints

The real train position should be within the error range of satellite positioning and inertial navigation positioning. Moreover, the coordinates of the real position must satisfy the trajectory equation of the railway line. Therefore, the constraints are as follows.

The constraint obtained from the positioning error of the Beidou satellite navigation system is as follows:

$$0 \leq ||pp(i, t) - sp(t)|| \leq e_s^{\max}, \tag{15}$$

where  $e_s^{\max}$  is the maximum distance error allowed by the Beidou satellite positioning system.

The constraints obtained from the distance error and the direction error of the inertial navigation system are as follows:

$$0 \leq ||pp(i, t) - s(t)|| \leq e_2^{\max}, \tag{16}$$

$$0 \leq ||\phi_{pp(i,t)s(t-1)} - \phi_t|| \leq e_3^{\max}, \tag{17}$$

where  $e_2^{\max}$  and  $e_3^{\max}$  are the maximum allowable distance error value and direction error value of the inertial navigation system, respectively.

The constraint obtained from the railway route trajectory equation is as follows:

$$\begin{cases} -0.5 \leq y - f_1(x) \leq 0.5, \\ -0.2 \leq z - f_2(x) \leq 0.2, \end{cases} \tag{18}$$

where  $f_1(x)$  and  $f_2(x)$  are the curve functions of  $y$  and  $z$ , respectively, at  $x$  fitted according to the accurate positioning points.

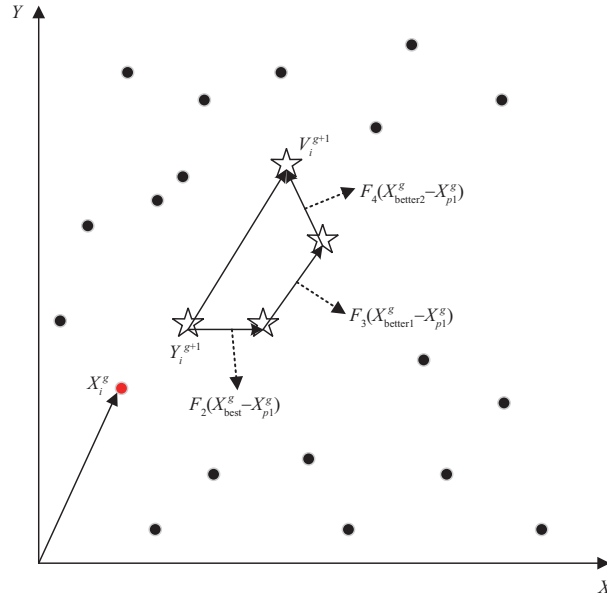


Figure 2 (Color online) Diagram of the improved variation operation.

**Remark 6.** At present, the gauge of a high-speed railroad is 1.435 m; the maximum error allowed on one side is 0.7175 m. A certain deviation will occur when the curve is fitted. If assuming the error range is 0.2 m, the allowable deviation will be 0.5175 m. Therefore, the plane error is set to  $\pm 0.5$  m. The height error of a high-speed railroad in the construction process is the millimeter level, which can be ignored. However, there are biases in the fitting results, so the height error is set to  $\pm 0.2$  m.

## 4 Positioning based on GWDE-MM algorithm

To integrate the electronic map information into the positioning process, this paper transforms the positioning problem into an optimization problem and proposes a GWDE-MM algorithm to solve the problem.

### 4.1 Improvement of the DE algorithm

The differential evolution algorithm is a population-based heuristic search algorithm [26, 27], which can avoid local optima to some extent. However, when solving complex optimization problems, the differential evolution algorithm may fall into a local optimum. To prevent this occurrence and expedite the solution of the algorithm, this paper improves the differential evolution algorithm by referring to the idea of the gray wolf algorithm [28]. The improvement method is as follows. On the basis of the original DE/current to best/1 variation strategy for the optimal value, two suboptimal solutions are retained. The individual performs the variation operation with simultaneous variation toward the optimal solution and two suboptimal solutions.

**Remark 7.** The gray wolf algorithm divides wolves into four classes, with the lower classes moving in the direction of the higher classes during predation. In the differential evolution algorithm, the DE/current to best/1 variation strategy proceeds as follows: a random variation is first performed to update the individual, and then a vector is added to it, which has a random size and is oriented toward the optimal value. This paper proposes to apply the idea of multiple optimal values in the gray wolf algorithm to the variation process of the differential evolution algorithm.

The variation strategy is shown in Figure 2.

The variation formula is as follows:

$$\begin{cases} X_i^g = (x_{i,1}^g, x_{i,2}^g, \dots, x_{i,d}^g), \\ Y_i^{g+1} = X_{p1}^g + F_1(X_{p2}^g - X_{p3}^g), \\ V_i^{g+1} = Y_i^{g+1} + F_2(X_{\text{best}}^g - X_{p1}^g) + V_i^{g+1} \\ \quad = Y_i^{g+1} + F_2(X_{\text{best}}^g - X_{p1}^g) + F_3(X_{\text{better1}}^g - X_{p1}^g) + F_4(X_{\text{better2}}^g - X_{p1}^g), \end{cases} \quad (19)$$

where  $X_i^g$  represents the  $i$ -th  $d$ -dimensional individual vector of the  $g$ -th generation in evolution.  $X_{\text{best}}^g$  is the optimal individual vector in the  $g$ -th generation population, and  $X_{\text{better1}}^g$  and  $X_{\text{better2}}^g$  are the two sub-optimal individual vectors in the  $g$ -th generation population.  $X_{p1}^g$ ,  $X_{p2}^g$ , and  $X_{p3}^g$  are three individuals randomly selected from the  $g$ -th generation population,  $p1 \neq p2 \neq p3$ , and the three individuals are not the optimal and sub-optimal individuals.  $Y_i^{g+1}$  represents the intermediate individual produced by the variation.  $F_1$ ,  $F_2$ ,  $F_3$ , and  $F_4$  are the scale factors of the variation operation,  $F_1$  is a random number generated between (0,0.5), and  $F_2$ ,  $F_3$ , and  $F_4$  are random numbers generated between (0,0.25).

## 4.2 Flow of the GWDE-MM algorithm

Map-matching algorithms mostly match the results of other positioning methods to electronic maps. To apply the electronic map information to the positioning process, this paper transforms the positioning problem into a multi-objective optimization problem and uses the GWDE-MM algorithm to locate high-speed trains. Before positioning, the positioning data collected by each positioning system must be preprocessed, then the orbit constraints are generated from the electronic map information, and the positioning is performed. The flow of the algorithm is shown in Figure 3.

The algorithm steps are as follows.

Step 1. Orbital equations are derived from the positioning coordinate data of a high-precision satellite navigation system: (1) filter out invalid data; (2) interpolate the electronic map data; and (3) establish appropriate orbit equations by data fitting.

Step 2. The positioning results are calculated from the measurements obtained from the satellite positioning systems and the inertial positioning systems. To unify the results of the two systems with the electronic map information in the same coordinate system, coordinate projection transformation is performed on the positioning results after filtering and eliminating invalid data.

Step 3. Initialize the population according to the proposed initialization formula. Then, set the population size  $N$ , the maximum number of iterations  $g_{\text{max}}$ , the crossover factor, and the variation factors  $F_1$ ,  $F_2$ ,  $F_3$ , and  $F_4$ .

Step 4. According to the designed fitness function, the fitness values of each individual are calculated, and then the optimal values  $X_{\text{best}}^g$  and two suboptimal values  $X_{\text{better1}}^g$  and  $X_{\text{better2}}^g$  are found by sorting.

Step 5. The GWDE-MM proposed in this paper is used to locate high-speed trains. The coordinates of the individual corresponding to the optimal value are output as the final matching positioning result.

Step 6. The obtained positioning results are fed back to the inertial navigation system and satellite positioning system, and the parameters of the two positioning systems are corrected.

Step 7. Repeat steps 2–6 until the train stops running.

## 5 Simulation and analysis

To validate the high-speed train positioning method proposed in this paper, a simulation experiment is designed based on MATLAB R2017b software. The simulation environment is a personal laptop with the following configuration: an x64-based operating system and an Intel(R) Core(TM) i5-6300HQ processor with 2.30 GHz CPU main frequency and 4 GB memory capacity. Experimental data are downloaded from the BeiDou Open Lab website. The experimental data include the actual position information of the vehicle, the velocity and acceleration information measured by the inertial navigation, and the latitude and longitude coordinate information of the Beidou satellite positioning. The sampling interval for data is 2 s, and the maximum satellite positioning error is 15 m.

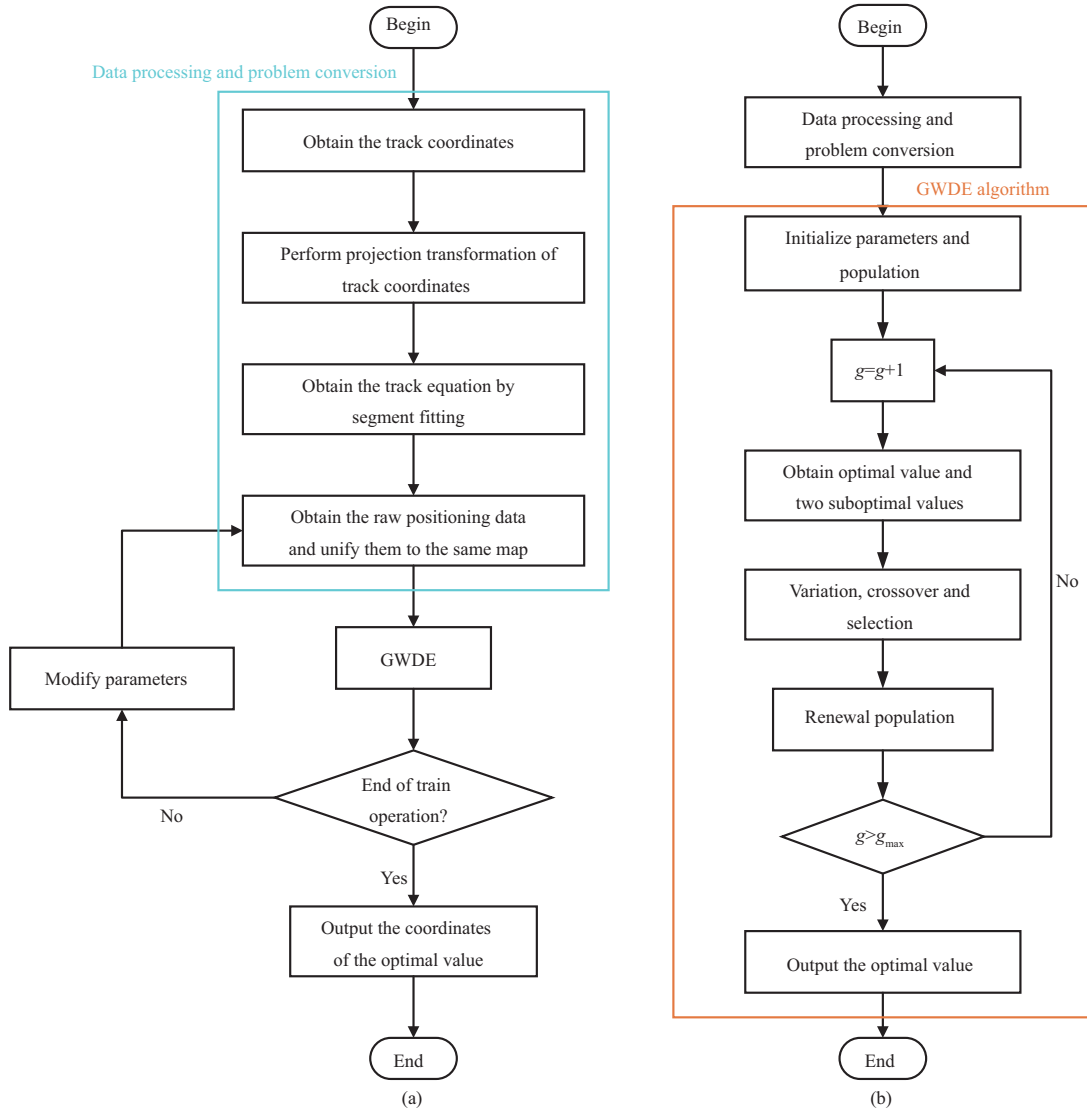


**Figure 3** (Color online) Flow charts of (a) the GWDE-MM algorithm positioning and (b) the GWDE algorithm.

### 5.1 Simulation method and experimental data

For experimental validation, 3-min positioning data are selected from all the positioning data for data simulation in this paper. In these data, the change in vehicle position in the  $X$ -,  $Y$ -, and  $Z$ -directions of the WGS84 coordinate system are 11624, 12126, and 7007 m, respectively.

**Remark 8.** The WGS84 coordinate system is created from coordinates observed by satellite observatories around the world, and it applies to the global positioning system of satellites.

The experimental data are divided into three parts in Figure 4: (1) orbital constraint equations derived from the coordinate transformation of map data; (2) direction and positioning information calculated from inertial navigation data by kinematics; and (3) positioning coordinates obtained by the projection transformation of latitude and longitude data provided by the satellite positioning system. Finally, after the positioning results obtained by the GWDE-MM algorithm, the best positioning result is output, and the parameters are corrected by the best positioning result.

Because the collected data do not belong to the same coordinate system and some data may be invalid, preprocessing of the raw data is required. After data processing, the three-dimensional distribution of the data in the WGS84 coordinate system is shown in Figure 5.

Figure 5 shows that large errors exist in the original positioning results of the inertial navigation system and the Beidou satellite navigation system. In addition, there are fluctuations in the positioning results

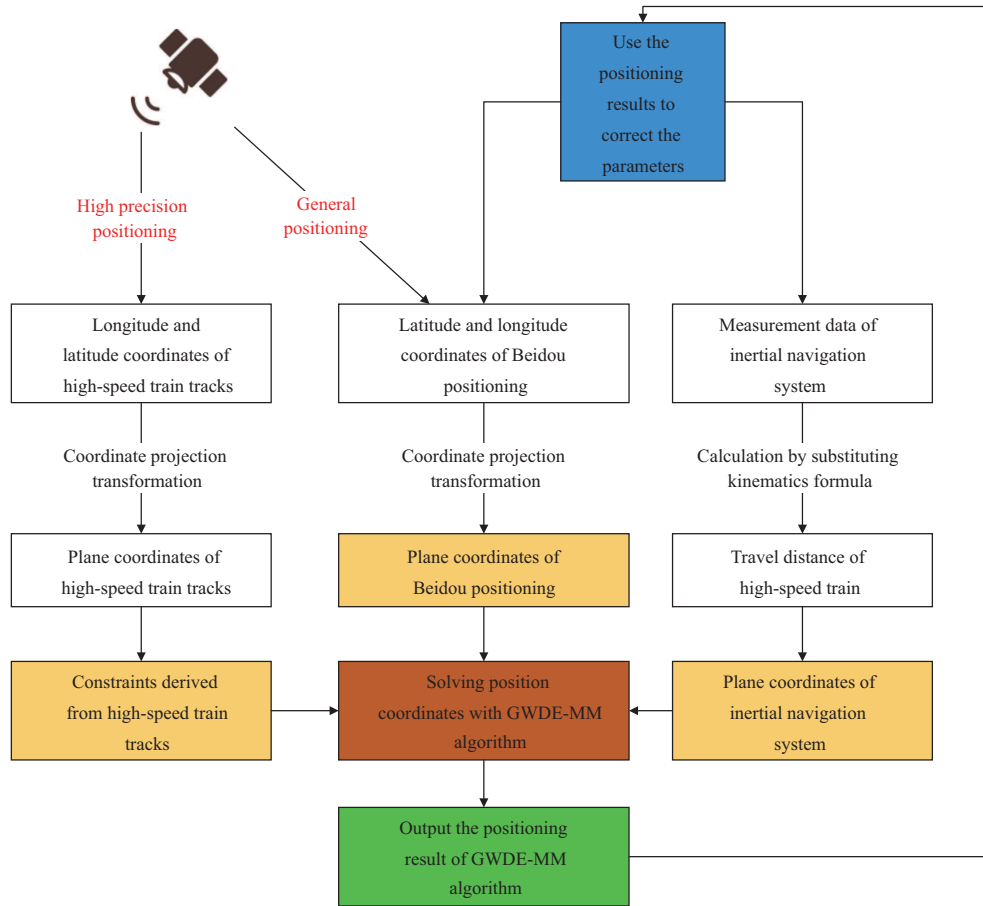


Figure 4 (Color online) Data frame diagram of the simulation experiment.

of the satellite navigation system. Therefore, the original positioning data need further processing to obtain more accurate positioning results.

## 5.2 Simulation results and analysis

### 5.2.1 Error analysis of the raw data

Figure 6 shows the error curve of the raw data. Figure 6(a) shows that the inertial navigation system has the disadvantage of accumulating errors, and the inertial navigation system cannot provide continuous and accurate positioning for a long time. Figure 6(b) shows that the results of the satellite positioning are fluctuating, which is caused by the perturbation of Beidou satellites and the selection of different positioning satellites.

Furthermore, the interference of satellite signal transmission in urban areas and tunnels may cause positioning failure of the satellite navigation system, so the combination positioning method is adopted for high-speed train positioning.

### 5.2.2 Fitting processing of the map data

In the positioning solution process based on the GWDE-MM algorithm, the electronic map information is added to the positioning process as an orbital constraint. The orbit equation derived from the coordinates of the electronic map must reasonably describe the orbit characteristics, which is an important factor in positioning accuracy. Based on the above reasons, this paper selects the fitting curve of a high-speed train track through the following comparison.

Taking the fitting results of the  $XY$ -plane as an example, the fitting results of the straight line segment are shown in Figure 7(a). As shown, the curve obtained by linear fitting cannot reasonably describe the train track, but the quadratic and cubic fitting results can reasonably describe the track curve. Figure 7(b) is a graph of the residual between the curve equation and the data points obtained by three fitting

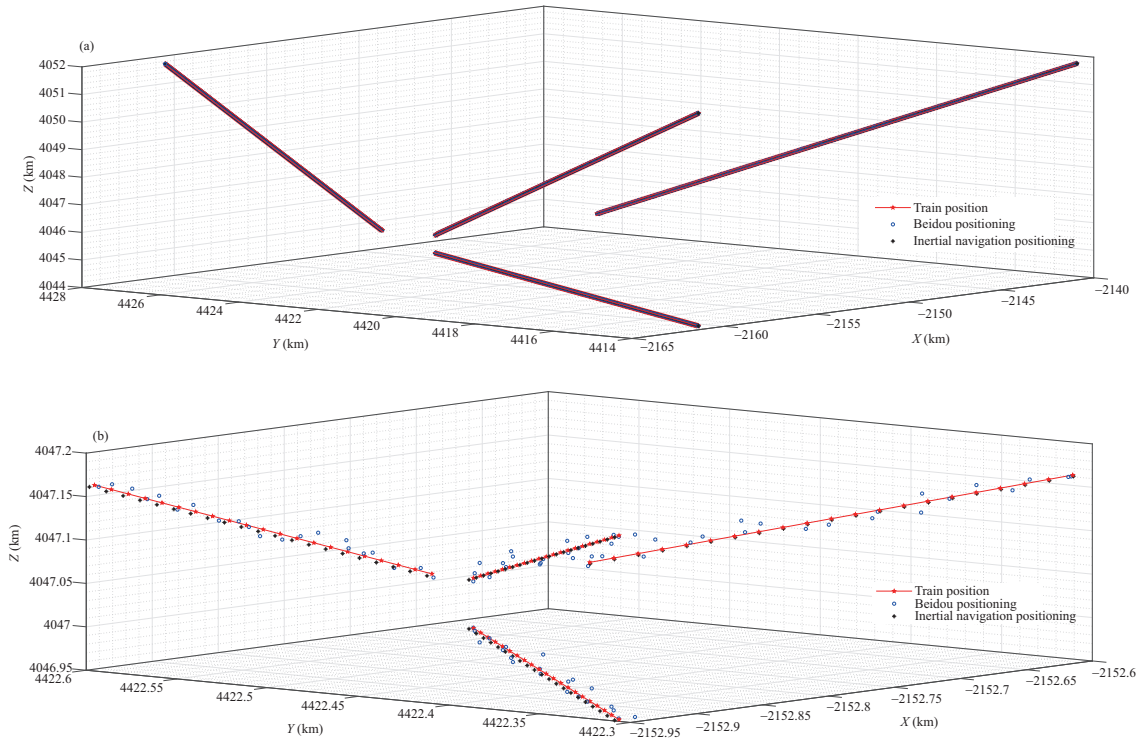


**Figure 5** (Color online) Three-dimensional distribution and planar projection of the raw positioning data. (a) Distribution of all data; (b) distribution of part data.

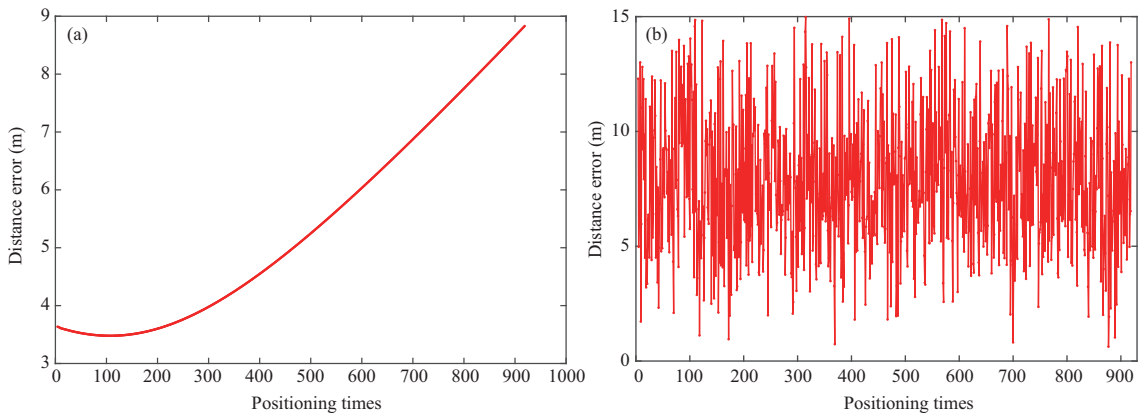


**Figure 6** (Color online) Error curves of the raw data. (a) The inertial navigation positioning; (b) Beidou positioning.

methods. The residual mode obtained by linear fitting is 0.10106, that by quadratic fitting is 0.00010581, and that by cubic fitting is 0.000012612. Therefore, the orbital equation obtained by quadratic fitting is chosen as a constraint equation for the GWDE-MM algorithm.

Figure 8(a) shows the curve fitting results of the XY-plane. Comparing and analyzing the results of the quadratic, cubic, and quartic fitting, fitting the road segment with the cubic curve is the best way to describe the road curve characteristics. Figure 8(b) shows that the residual moduli of the three fitting methods are 0.0049097, 0.0021963, and 0.0026006, respectively. The cubic fitting has the smallest residual modulus. In summary, the result of the cubic fitting for this curve segment is closest to the actual route characteristics. Therefore, this result is used as the constraint equation later.

### 5.2.3 Error analysis of the positioning results

Figure 9 shows the partial positioning results of the GWDE-MM algorithm. Comparing Figure 9 with Figure 5, the positioning results of the GWDE-MM algorithm are closer to the actual location than the satellite positioning results. The positioning results of the GWDE-MM algorithm no longer need map-

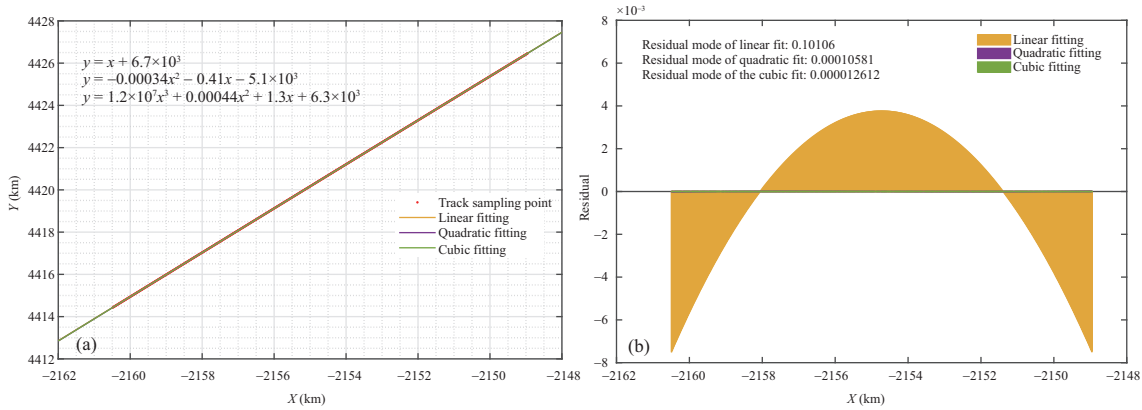


**Figure 7** (Color online) Comparison chart of the linear map data fitting results. (a) Fitting curves of the linear map data; (b) fitting residuals of the straight line part.

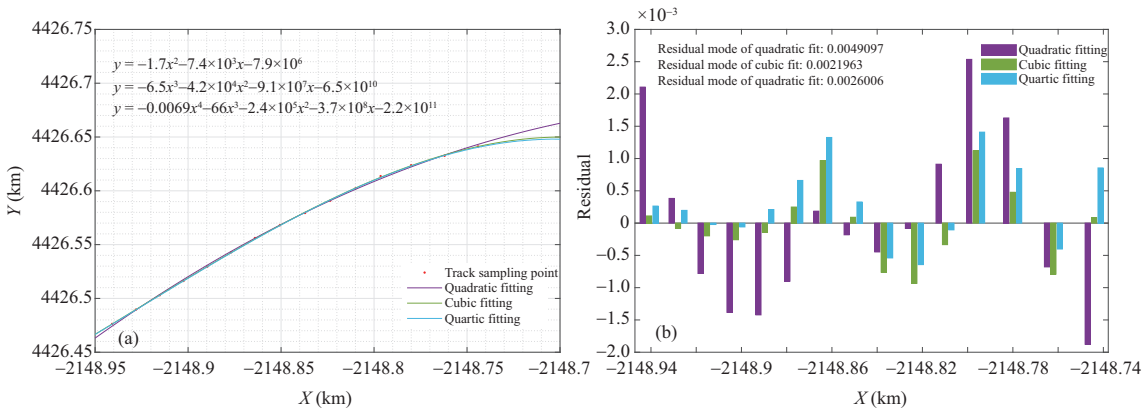


**Figure 8** (Color online) Comparison chart of the curve map data fitting results. (a) Fitting curves of the curve part; (b) fitting residuals of the curve part.

matching. Thus, the feasibility of the GWDE-MM algorithm to solve the train positioning problem is proven.

This experiment shows the superiority of the GWDE-MM algorithm by comparing its positioning errors and solution time to those of the DE-MM algorithm. To compare and analyze the positioning efficiency, the solution time of 20 groups of positioning data is selected from 910 groups of positioning data in this experiment. The results are as follows.

For the multi-objective optimization problems mentioned in this paper, Table 1 compares the solving speed of the two algorithms in terms of the average solution time, maximum solution time, and minimum solution time. Similarly, the positioning errors of the two algorithms are compared in Table 2. The comparison results show that the improvement accelerates the solving speed of the algorithm and prevents the algorithm from falling into a local optimum. The solving speed and the reliability of train positioning are improved.

Table 3 compares and analyzes the positioning effect before and after the algorithm improvement based on the distribution of the positioning error values. The analysis results show that before algorithm improvement, 487 results had a positioning error within 4 m, accounting for 53.5% of the total number of positions. After the improvement, 594 results had a positioning error within 4 m, accounting for 65.3% of the total number of positions. After improvement, the number of errors within 4 m increased by 107 or 11.8%. Table 3 shows that the improved algorithm has better positioning results and can locate high-speed trains more accurately.

In Figure 10, the red polyline is the original satellite positioning error. The blue polyline is the positioning error obtained with the DE-MM algorithm. The green polyline is the positioning error obtained with the GWDE-MM algorithm. Combining Table 3 and Figure 10, the error obtained by the GWDE-MM algorithm is smaller. The GWDE-MM algorithm has smaller maximum and average positioning errors, although its minimum positioning error is larger than the DE-MM algorithm.

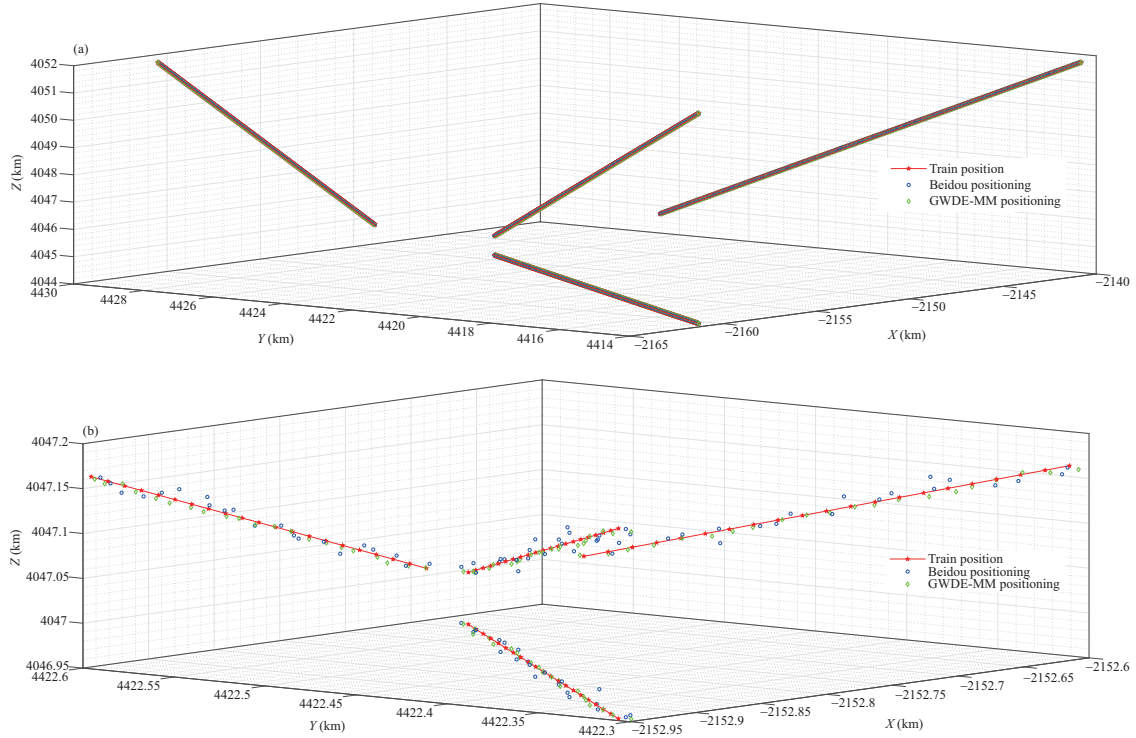


**Figure 9** (Color online) Three-dimensional distribution and planar projection of the positioning results. (a) Distribution of all data; (b) distribution of part data.

**Table 1** Comparison of the time required for positioning algorithms

Solving algorithm	Average time (s)	Maximum time (s)	Minimum time (s)
DE-MM	0.1305787	0.393426	0.098023
GWDE-MM	0.107531105	0.128569	0.091722

**Table 2** Comparison of the algorithm positioning errors

	Average error (m)	Maximum error (m)	Minimum error (m)	SD (m)
Original error	7.859	14.98	0.6249	3.041
DE-MM	3.836	9.783	0.1138	1.525
GWDE-MM	3.649	8.635	0.1882	1.467

**Table 3** Comparison of the positioning errors

Solving algorithm	Error: 0–1 m	Error: 1–2 m	Error: 2–4 m	Error: 4–6 m	Error $\geq$ 6 m	Total times
DE-MM	8	95	384	319	105	911
GWDE-MM	16	114	464	274	43	911

In this paper, the electronic map information is transformed into an orbit constraint equation and incorporated into the positioning process. Whether this idea can improve positioning accuracy is discussed in a simulation experiment. The positioning error analysis of the two methods is shown in Figure 11 and Table 4.

The positioning errors of the two algorithms are compared in Table 4. As shown in Table 4, the positioning results of the GWDE-MM algorithm are significantly better than those obtained by matching the GWDE positioning with the map-matching method. Thus, the positioning accuracy is improved by the GWDE-MM algorithm, which incorporates the electronic map as a constraint in the combined positioning process.

In Figure 11, the red polyline is the original satellite positioning error. The blue polyline is the positioning error obtained by matching the result of the differential evolution algorithm based on the gray wolf algorithm (GWDE). The green polyline is the positioning error obtained by using the GWDE-MM algorithm.

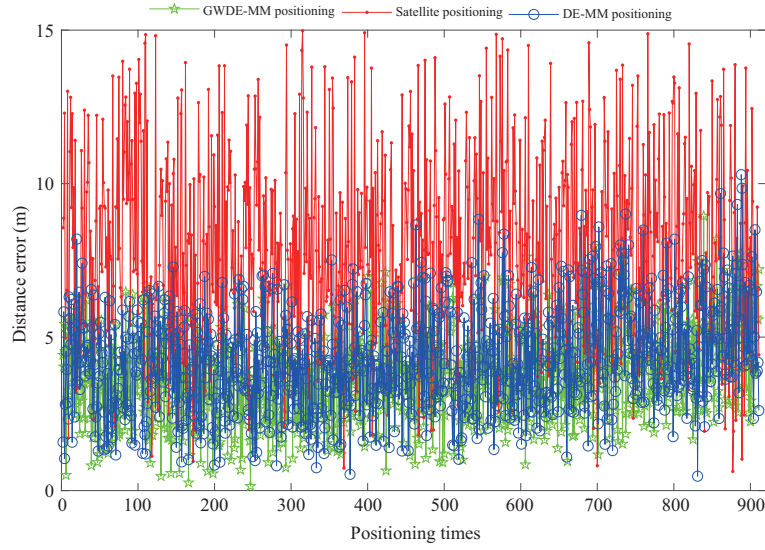


**Figure 10** (Color online) Comparison chart of the GWDE-MM and DE-MM algorithms.

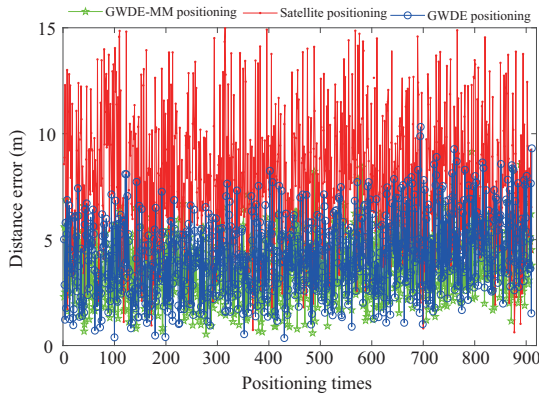


**Figure 11** (Color online) Comparison chart of the GWDE-MM and GWDE algorithms.

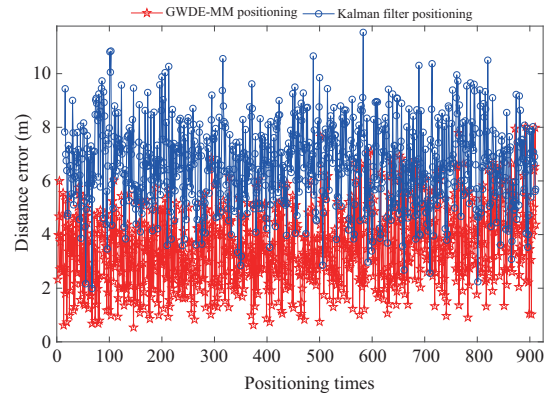


**Figure 12** (Color online) Comparison chart of the GWDE-MM and Kalman filter algorithms.

**Table 4** Comparison of the algorithm positioning errors

	Average error (m)	Maximum error (m)	Minimum error (m)	SD (m)
Original error	7.859	14.98	0.6249	3.041
GWDE	4.306	10.31	0.301	1.694
GWDE-MM	3.649	8.635	0.354	1.467

According to Figure 11 and Table 4, the GWDE-MM algorithm performs better in 910 positioning results, regardless of minimum, maximum, or average positioning errors. Overall, the results obtained by adding electronic maps to the positioning process are closer to the real positioning, and the positioning error fluctuations are smaller.

To further demonstrate the superiority of the GWDE-MM algorithm, this paper designs a comparative experiment of the Kalman filter and GWDE-MM algorithms under the same environment. The Kalman filter algorithm used in these experiments refers to the design of the train positioning information fusion algorithm in [29], and the experimental results are shown in Figure 12 and Table 5.

As Figure 12 shows, the GWDE-MM algorithm has significantly better positioning results than the Kalman filter algorithm. The data comparison in Table 5 also clearly proves that the GWDE-MM algorithm is superior in terms of maximum, minimum, and average errors. In summary, the GWDE-MM algorithm is more advantageous than the Kalman filter algorithm in solving the multi-target positioning problem of high-speed trains.

**Table 5** Comparison of the algorithm positioning errors

Solving algorithm	Average error (m)	Maximum error (m)	Minimum error (m)	SD (m)
Kalman filter	6.617	11.54	1.99	1.521
GWDE-MM	3.649	8.635	0.1882	1.467

## 6 Conclusion

In this paper, the high-speed train positioning problem was transformed into a multi-objective optimization problem with constraints. At the same time, the orbit constraint equation was obtained by fitting the electronic map information. With this method, map-matching was incorporated into the positioning process. The differential evolution algorithm for solving the optimization problem was improved. Through theoretical and column analysis, the following conclusions are drawn.

(a) It is feasible to transform the positioning problem into a multi-objective optimization problem with constraints and solve the positioning problem by using the GWDE-MM algorithm.

(b) The improvement in the differential evolution algorithm can increase the solving speed of the proposed multi-objective optimization problem and avoid local optima. The new algorithm enhances the real-time performance and reliability of high-speed train positioning.

(c) The method of fitting the electronic map information to the track constraint equation improves the accuracy of the high-speed train positioning.

This study will further investigate how to achieve faster and more accurate high-speed train positioning by designing more reasonable objective functions and variation factors in the improved variation strategy.

**Acknowledgements** This work was supported by National Natural Science Foundation of China (Grant Nos. U2034211, 61903141, 61733005), Joint Opening Foundation of State Key Laboratory of Synthetical Automation for Process Industries (Grant No. 2022-KF-21-03), and Technological Innovation Guidance Program of Jiangxi Province (Grant No. 20203AEI009).

## References

- Li W D, Hou L H. Research on high-speed train positioning technology based on satellite navigation system (in Chinese). *Inform Control*, 2016, 45: 479–486
- Yang G, Lin Y. Train positioning method based on multi-sensor information fusion (in Chinese). *Railway Signalling & Commun*, 2019, 55: 42–47
- Duan Z Q, Liu J Y, Li X, et al. Research of train positioning method by balise-and-SINSs information fusion (in Chinese). *Railway Signalling Commun*, 2020, 56: 1–6
- Luo Y, Wu W Q, Babu R, et al. A double-filter-structure based COMPASS/INS deep integrated navigation system implementation and tracking performance evaluation. *Sci China Inf Sci*, 2014, 57: 012206
- Zhang C D, Wang Z R. Integrated positioning method based on SINS/RFID of high-speed trains in long tunnel (in Chinese). *Comput Simul*, 2020, 37: 124–128, 188
- Li W D, Hou L H, Wang Y S. Research on location method of combined train based on BDS/GSM-R (in Chinese). *J Railway Sci Engin*, 2016, 13: 552–556
- Borenovic M, Neskovic A, Neskovic N. Vehicle positioning using GSM and cascade-connected ANN structures. *IEEE Trans Intell Transp Syst*, 2013, 14: 34–46
- Yang Y, Chen G W, Wang J W, et al. Research on train combination positioning method based on grey neural network (in Chinese). *J Measurement Sci Instrum*, 2019, 10: 143–149
- Liu F, Guo Y, Zheng X, et al. Study on map matching method based on geometric features of road (in Chinese). *Navigat Position Timing*, 2020, 7: 67–72
- Li X, Zhao H B, Ma S G. Study of fine alignment scheme of in-vehicle SINS based on map-matching (in Chinese). *Navigat Control*, 2020, 19: 52–58
- Kim K, Seol S, Kong S H. High-speed train navigation system based on multi-sensor data fusion and map matching algorithm. *Int J Control Autom Syst*, 2015, 13: 503–512
- Liu J, Li K, Fu L Z, et al. A map matching algorithm based on track constraint characteristics (in Chinese). *Railway Commun Signals*, 2020, 56: 7–10
- Yuan Y S, Lyu J Y. Research on train positioning system based on map matching and multi-information fusion. In: *Proceedings of IEEE 6th International Conference on Computer and Communications (ICCC)*, 2020. 2271–2275
- Jiang W, Chen S R, Cai B G, et al. A multi-sensor positioning method-based train localization system for low density line. *IEEE Trans Veh Technol*, 2018, 67: 10425–10437
- Guo Z H. Research and implementation of train positioning visualization technology based on GIS. Dissertation for Master's Degree. Chengdu: Southwest Jiaotong University, 2017
- Wang X, Yao L B. Application of Lambert projection in survey on high-speed railway (in Chinese). *Railway Survey*, 2014, 40: 17–19
- Liu J, Lu J H, Yang X Y, et al. Deformation analysis of Lambert projection and Gauss-Krueger projection in mid-latitude area (in Chinese). *Survey Map Geology Mineral Res*, 2019, 35: 12–14, 17
- Karimi H, Conahan T, Roongpiboonsopit D. A methodology for predicting performances of map-matching algorithms. In: *Proceedings of International Symposium on Web and Wireless Geographical Information Systems*. Berlin: Springer, 2006. 202–213
- Li D Q, Wang Y, Liu L. The design and implementation of a map matching algorithm (in Chinese). *Navigat Position Timing*, 2017, 4: 31–34

- 20 Dixit A, Mani A, Bansal R. An adaptive mutation strategy for differential evolution algorithm based on particle swarm optimization. *Evol Intel*, 2022, 15: 1571–1585
- 21 Wang Y K, Chen X B. Hybrid quantum particle swarm optimization algorithm and its application. *Sci China Inf Sci*, 2020, 63: 159201
- 22 Hu Y, Wang J, Liang J, et al. A self-organizing multimodal multi-objective pigeon-inspired optimization algorithm. *Sci China Inf Sci*, 2019, 62: 070206
- 23 Cheng S, Lei X J, Lu H, et al. Generalized pigeon-inspired optimization algorithms. *Sci China Inf Sci*, 2019, 62: 070211
- 24 Zhang X, Zhang Y, Ming Z. Improved dynamic grey wolf optimizer. *Front Inform Technol Electron Eng*, 2021, 22: 877–890
- 25 Gu Y L, Lu W Q, Shao Z Z. Multi-objective genetic algorithm-based map-matching method for floating car data (in Chinese). *J Beijing Univ Technol*, 2019, 45: 585–592
- 26 Yang Y, Chen R Q, Yu J S. Study on differential evolution-particle swarm optimization based hybrid optimization algorithm and its application (in Chinese). *Comput Eng Appl*, 2010, 46: 238–241
- 27 Tassing R, Guo L, Liu J, et al. Gene sorting in differential evolution with cross-generation mutation. *Sci China Inf Sci*, 2011, 54: 268–278
- 28 Mirjalili S, Mirjalili S M, Lewis A. Grey wolf optimizer. *Adv Eng Software*, 2014, 69: 46–61
- 29 Li W D, Yu Y, Wang Y M, et al. Information fusion algorithm of train positioning based on sequence-assisted adaptive fading UKF (in Chinese). *J Railway Sci Eng*, 2022, 19: 1838–1844